Title	Mesoporous titania nanotubes: their preparation and application as electrode materials for rechargeable lithium batteries
Authors	Wang, Kaixue;Wei, Mingdeng;Morris, Michael A.;Zhou, Haoshen;Holmes, Justin D.
Publication date	2007-09-06
Original Citation	Wang, K., Wei, M., Morris, M. A., Zhou, H. and Holmes, J. D. (2007) 'Mesoporous Titania Nanotubes: Their Preparation and Application as Electrode Materials for Rechargeable Lithium Batteries', Advanced Materials, 19(19), pp. 3016-3020. doi: 10.1002/adma.200602189
Type of publication	Article (peer-reviewed)
Link to publisher's version	https://onlinelibrary.wiley.com/doi/10.1002/adma.200602189 - 10.1002/adma.200602189
Rights	© 2007 WILEY-VCH Verlag GmbH & Co. KGaA, Weinheim. This is the pre-peer reviewed version of the following article: (2007), Mesoporous Titania Nanotubes: Their Preparation and Application as Electrode Materials for Rechargeable Lithium Batteries. Adv. Mater., 19: 3016-3020, which has been published in final form at https://onlinelibrary.wiley.com/doi/epdf/10.1002/adma.200602189. This article may be used for non-commercial purposes in accordance with Wiley Terms and Conditions for Self-Archiving
Download date	2024-05-03 16:15:04
Item downloaded from	https://hdl.handle.net/10468/8143

Mesoporous Titania Nanotubes: Their Preparation and Application as Electrode Materials for Rechargeable Lithium Batteries **

By Kaixue Wang [+], Mingdeng Wei [+], Michael A. Morris, Haoshen Zhou*, and Justin D. Holmes*

[*]Dr. J. D. Holmes, Dr. K. Wang, Prof. M. A. Morris
Materials Section & Supercritical Fluid Centre
Department of Chemistry
University College Cork
Cork (Ireland)
Fax: (+353) 21-4274097
Email: j.holmes@ucc.ie

Dr. H. Zhou,
Institute of Energy Technology
National Institute of Advanced Industrial Science and Technology (AIST)
Umezono 1-1-1, Tsukuba, 305-8568 (Japan)
Fax: (+81) 298-615-829
E-mail: hs.zhou@aist.go.jp

Dr. M. D. Wei
Japan Science and Technology Agency (JST)
Light and Control Research Group
PRESTO, Kawaguchi
Saitama 3320012 (Japan)

[+]These authors contribute to this work equally.

[**]We gratefully acknowledge the financial support from Science Foundation Ireland (Grant number: 03/IN3/I375). K. W. thanks Dr. Xueyan Wu for kindly supplying the 50 nm AAO membranes. Supporting information is available online at Wiley InterScience or from the author.

Mesoporous titania and titania nanotubes, with high surface-to-volume ratios, have recently been reported to demonstrate improved properties compared to colloids, films and other forms of titania in applications such as photocatalysts,[1, 2] gas sensors,[3] photovoltaic cells[4-6] and rechargeable lithium batteries.[7-10] Therefore, particular attention has been paid to the preparation of titania

nanotubes, or arrays of tubes, and many methods have been developed including the hydrothermal treatment of TiO_2 nanoparticles with alkali solution,[11-13] anodization of titanium foil,[14, 15] deposition of sol-gels within templates [16-18], hydrolysis of TiF_4 under acidic conditions,[19] sonication of titania particles in aqueous NaOH solution,[20] and surfactant-assisted templating methods.[21, 22] Materials with mesoporous structures possess an extraordinarily high surface area. The synthesis of titania nanotubes, with mesoporous walls and hence high surface areas, will be invaluable for all applications employing the wide band gap semiconductor. Therefore, there is a requirement for the development of a facile and reproducible way to prepare titania nanotubes with well-defined mesoporous wall structures. We have previously shown that one-dimensional mesoporous silica nanotubes and nanowires can be fabricated inside the pores of anodic aluminum oxide (AAO) membranes.[23] Recently, Chae et al. reported the preparation of titania nanofibres with wormhole-like mesoporous structure using AAO as a 'hard template'.[24] Even though mesoporous SiO_2 nanotubes and titania nanofibres have been prepared, the fabrications of TiO_2 nanotubes with well ordered mesopores are still a challenge because of the complexity of sol-gel chemistry. Herein, we report the preparation of titania nanotubes with mesoporous walls within AAO membranes and their application in a high rate rechargeable lithium battery. Well-aligned titania nanotube arrays were fabricated via a drying process utilizing supercritical CO_2 after the dissolution of the membranes. These mesoporous titania nanotubes, with a 3-dimensional (3 D) network structure, were investigated as the electrode material of a rechargeable lithium battery. The structure of the mesoporous nanotubes was specifically designed to allow efficient transport of both lithium ions and electrons, which are necessary for a high rate rechargeable battery. The experimental results obtained proved that the mesoporous nanotube structure plays an important role in the efficiency of the high rate performance of the battery.

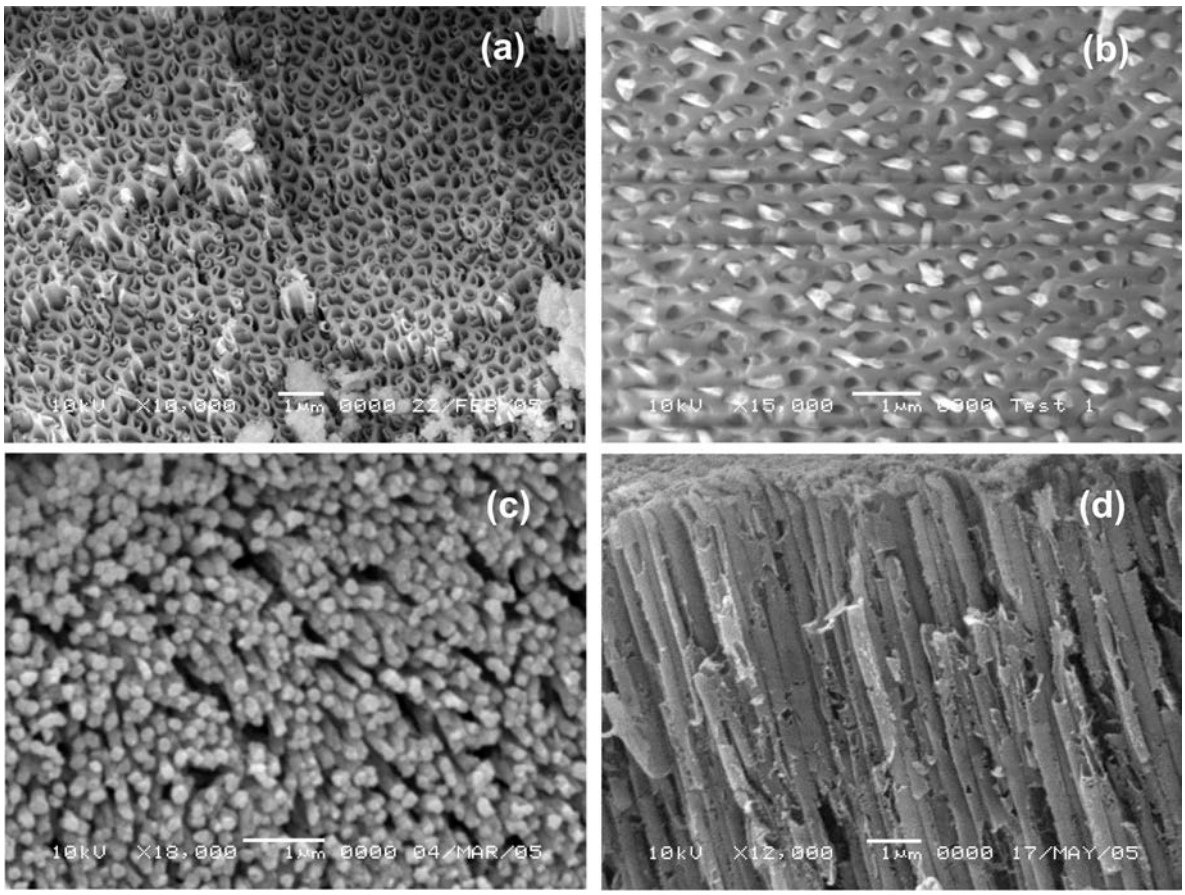

Figure 1 Scanning electron microscope images of titania nanotubes produced within (a) 0.2 and (b) 0.1 μm AAO membranes after annealed at 150 ºC, and (c) top and (d) side view of nanotube arrays prepared by a supercritical CO_2 drying process following the dissolving of AAO.

Scanning electron microscope (SEM) images of the titania nanotubes annealed at 150 ºC are shown in Figure 1. Well-defined nanotubes are observed occupying most of the pores of the AAO. The size and uniformity of the nanotubes fabricated by this templating method are closely related to the pore size and quality of the alumina membranes employed.[17] Nanotubes prepared within a 0.2 μm Whatman AAO membrane have an outer diameter of approximately 200 nm and wall thickness of approximately 30 nm, which are uniform over the entire surface of the membrane as shown in

Figure 1a. By choosing alumina membranes with relatively small pores, titania nanotubes with diameters with mean diameters of less than 100 nm can be fabricated. Figure 1b shows the titania nanotubes with outer diameters of approximately 100 nm embedded inside a 0.1 μm Whatman AAO membrane. In our experiments, the AAO membranes were totally submerged into the precursor sol. The viscosity of the sol was relatively low, about 0.008 cP after dilution by ethanol, allowing the sol to penetrate through the alumina membranes by capillary forces and as a result the pore channels of the membranes were completely occupied by the precursor sol. The densification and gelation of the precursor sol occurs with the evaporation of ethanol during the various aging periods. Due to an affinity between the formed gel and the hydrophilic alumina walls, further shrinkage of the gel occurs in a direction perpendicular to AAO pore channels,[23, 25] which finally results in the formation of titania nanotubes during further aging and calcination. Moreover, by increasing the viscosity of the sol to values over 0.025 cP, instead of nanotubes mesoporous titania nanorods can be prepared by this in-sol aging method (see the supporting information).

The nanotubes embedded in the pores of the AAO membranes are highly ordered and vertically aligned arrays. However, after removal of the AAO template, by dissolving in a NaOH solution, the well-aligned nanotubes aggregate together into an entangled mass due to surface tension forces acting on the nanotubes during the drying process (see the supporting information). To avoid the entanglement of the nanotubes a supercritical fluid drying process, employing supercritical carbon dioxide (sc-CO_2), which has successfully been used to prepare free-standing CdS nanowire arrays[26], was used. As shown in the SEM images in Figure 1c and d, large area, well-ordered nanotube arrays are formed after the sc-CO_2 drying process. These nanotube arrays do not entangle and retain their vertical alignment, which will greatly benefit their incorporation into

device structures.

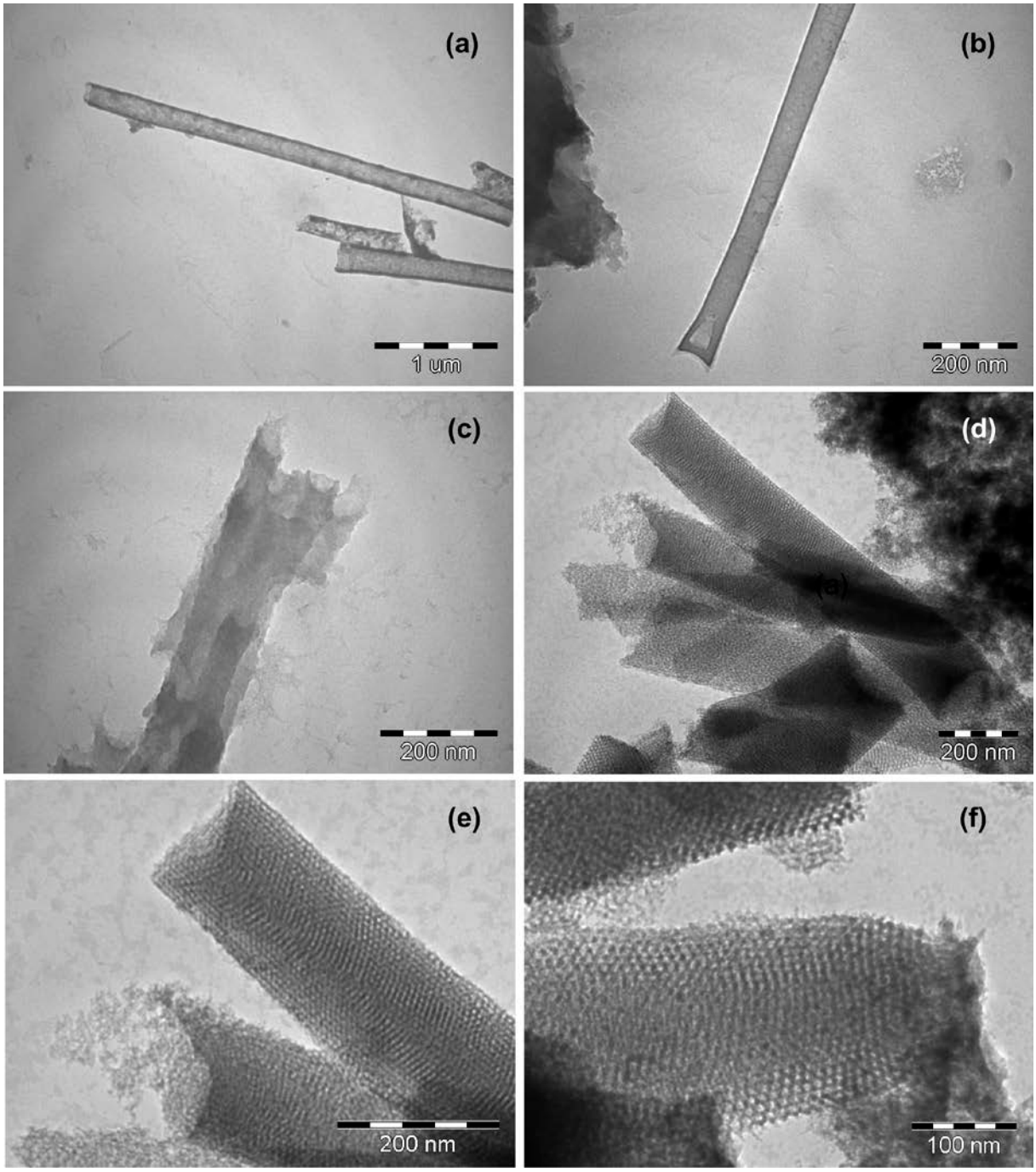

Figure 2. Transmission electron microscopy images of 150 ºC calcined TiO_2 nanotubes or tube bundle with outer diameter of approximately (a) 200, (b) 100, and (c) 50 nm prepared using 0.2, 0.1 and home-made 0.05 μm AAO membranes as hard templates, respectively, and (d, e and f) side view of 450 ºC calcined nanotubes showing the hexagonal-ordered mesoprous structure.

Transmission electron microscopy (TEM) images of the TiO_2 nanotubes after removal of the

alumina matrix are presented in Figure 2. Figure 2a-c shows a representative low-magnification TEM images of the 150 °C calcined titania nanotubes, which were prepared using AAO membranes with different pore diameters as templates. The diameter and length of the titania nanotubes prepared mainly depends on the porous nature of the alumina membranes. Thus, the dimensions of the nanotubes prepared by this sol-gel method can be manipulated by simply choosing AAO membranes with different pore size. Our results are consistent with the structural nature of the commercial Whatman anodic membranes and the fact that the pore enlargement of AAO in the acidic sol is inevitable during the aging process. Employing a 50 nm home-made AAO as a template, titania nanotubes with dimension less than 50 nm are successfully produced as shown in Figure 2c. The mesoporous nature of these nanotubes, when calcined at 450 ºC for more than 3 hours, is confirmed by TEM as shown in Figure 2d-e. The mesopores in the tube walls are hexagonal-packed and predominately perpendicular to the longitudinal axis of the tube, which is also observed for the meso-structured silica in AAO membranes, as previously reported by Yang *et al*..[27] The coexistence of macroporous tube channels and the mesoporous wall suggests that the synthesized mesoporous titania nanotubes have a 3D network structure. The mean mesopore diameter is approximately 7.5 nm, which is in the same range as the pore diameter of mesoporous nanofibres and nanorods prepared using the same copolymer surfactant templates. [28] The preservation of the ordered mesopores after calcination at a temperature of 450 ºC suggests that these mesoporous tube structures are thermally stable. After annealing at 150 ºC, the mesoporous walls of the titania nanotubes are still amorphous with surfactant molecules inside the mesopores. Calcination at a temperature of 450 °C leads to the decomposition of surfactant molecules and the crystallization of the amorphous walls. The high-angle PXRD pattern of a mesoporous titania nanotube sample, calcined 450 °C, shows six well-resolved broad diffraction peaks located at 25.4,

38.0, 48.1, 54.0, 54.9 and 62.7° (2θ), which can be readily assigned to (101), (004), (200), (105), (211) and (204) diffraction planes respectively of the anatase phase (JCPDS No. 84-1286) (see the supporting information). PXRD studies suggest that the inorganic framework of these nanotubes is predominantly composed of nanosized anatase crystallines.

The mesoporous nature of the titania nanotubes was further confirmed by Brunauer-Emmet-Teller (BET) measurements conducted at 77 K. As a piece of AAO membrane can only produce a very small quantity of titania nanotubes, it is quite difficult to prepare a large quantity of nanotubes or nanofibres required by BET analysis. In order to satisfy the quantity requirement by BET measurement, more than 100 pieces of 0.2 μm AAO membranes were used in the preparation of titania nanotubes in this work. Pure titania nanotubes were obtained by dissolving the AAO membranes in a 2.0 M NaOH solution after the samples were calcined at a temperature of 450 ºC for more than 3 hours. N_2 adsorption-desorption isotherms, as shown in Figure 3 for the pure titania nanotubes, reveals the presence of the multi-modal porosity mesopores together with macropores. The isotherms at a relative pressure of 0.45~0.6 can be classified as type IV, typical of mesoporous materials. The adsorption and desorption activity at high relative pressure, implying the presence of macropores, [29] derives from the large pore channels of the titania nanotubes. The narrow hysteresis loop at a low relative pressure indicates that the porous structure is quite open and there is no significantly delay in the capillary evaporation with respect to the capillary condensation of nitrogen.[30] BET surface area and total pore volume are 400 m^2g^{-1} and 0.94 cm^3g^{-1}, respectively. The BJH pore diameter distribution plot has a broader distribution compared to the mesoporous titania powders. The average pore diameter of the mesopores is approximately 7.6 nm, which is good agreement with the TEM observation. The increase in pore

volume with pore diameter over 10 nm can be related to the macroporous channels of the nanotubes. This phenomenon was reported previously in the preparation of multi-scale porous transition-metal oxide spheres. [29]

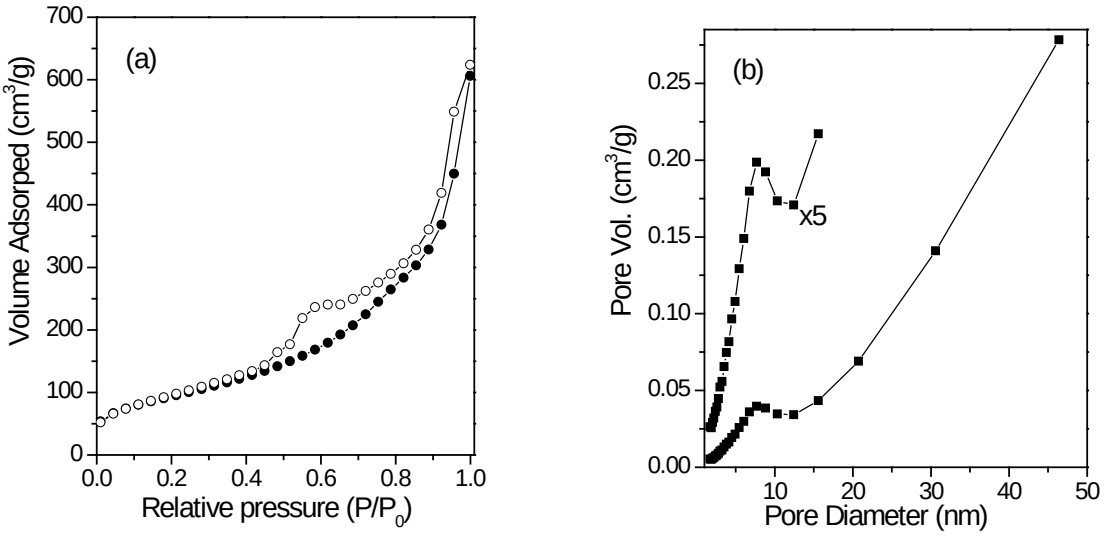

Figure 3 (a) Nitrogen adsorption-desorption isotherm plots and (b) pore size distribution curve for 450 ºC calcined mesoporous TiO_2 nanotubes prepared by using 0.2 μm AAO membranes as templates.

Recently, nanostructure materials, especially periodic mesoporous active electrode materials, have shown remarkable promise for improving the specific capacities, cycle stability and performance rate of the rechargeable lithium battery.[7, 19, 31] In particular, the thin walls of mesoporous materials allow lithium ions to diffuse along the pores and through the pore walls, i.e. in two directions, significantly shortening the diffusion path for the ion. However, it is still a challenge to decrease an electron's diffusion length in an active material. In this work, the mesoporous nanotubes were designed to provide efficient lithium ion and electron transport paths. The wall thickness of the nanotubes investigated was approximately 30 nm, which allowed electrons from the ketylene black carbon (KB), adsorbed onto the outer surface of the mesoporous TiO_2 nanotubes, to be quickly transported into TiO_2 framework and undergo a charge-discharge reaction.

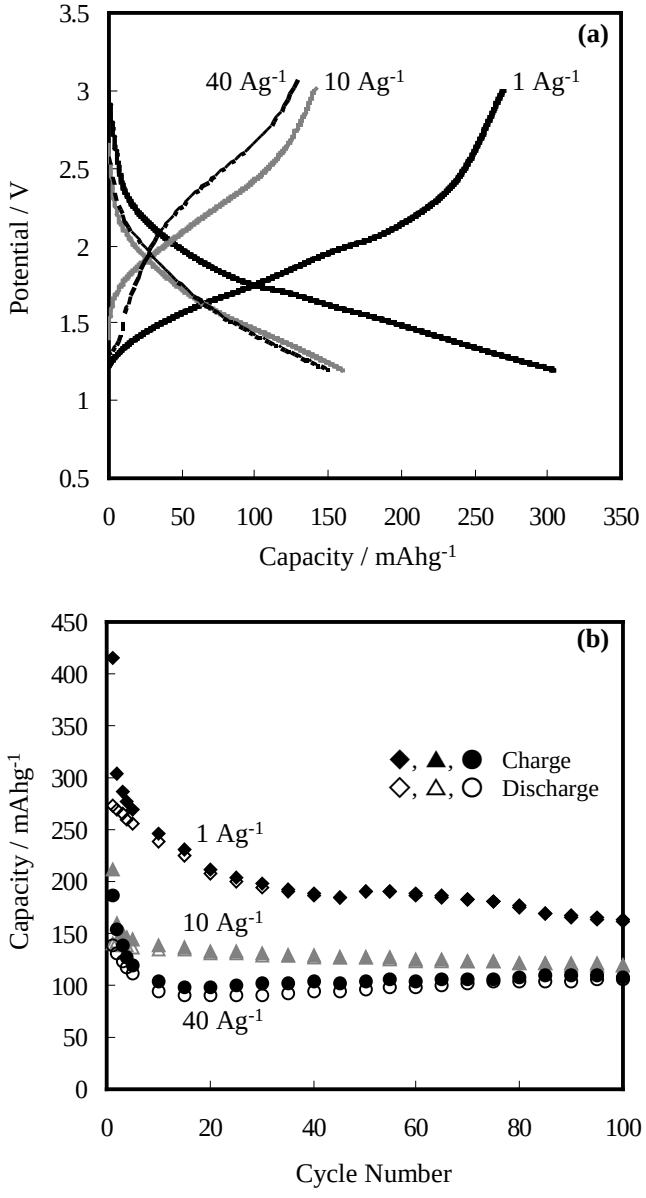

Figure 4 (a) The second cycle charge-discharge profiles of the mesoporous titania nanotube in the potential range from 1.2 to 3.0 V (versus Li^+/Li) with the current densities of 1, 10, and 40 Ag^{-1} based on active TiO_2. (b) The performance cycle of charge and discharge capacities of mesoporous titania nanotube at the current densities of 1, 10 and 40 Ag^{-1}.

Figure 4a shows the second cycle charge-discharge profiles of mesoporous titania nanotubes in the potential range from 1.2 to 3.0 V (Li^+/Li) with current densities of 1, 10 and 40 Ag^{-1}. Specific capacities of 303, 160 and 150 $mAhg^{-1}$ were obtained at current densities of 1, 10 and 40 Ag^{-1}, respectively. In the electrochemical measurements, KB powder was used as the conductive assistant material. Thus, the specific capacity of pure KB was also measured under the same conditions. The pure KB powder showed capacities of approximately 14 and 2.5 $mAhg^{-1}$ for current densities of 1 and 10 Ag^{-1}, respectively (see Supporting Information). The capacity of KB at a current density of 40 Ag^{-1} was too small to be detected. Hence for our samples, the actual capacities of the mesoporous titania nanotubes were ca. 289, 157.5, and 150 $mAhg^{-1}$, corresponding to x = 0.86, 0.47 and 0.45 for Li_xTiO_2, respectively. The x = 0.86 for Li_xTiO_2 is much larger than 0.5 reported in ordinary anatase.[32] This large specific capacity resulted from the high surface area of nanostructure materials and has been previously observed in mesoporous TiO_2 and TiO_2 nanoparticles.[7-10, 33] For the mesoporous nanotubes, a remarkable specific capacity of 150 $mAhg^{-1}$ was obtained even at a current density of 40 Ag^{-1} (about 240 C). The high rate of charge-discharge is attributed to the 3 D network structure of the mesoporous nanotubes.

It can be seen from the Figure 4b that mesoporous titania nanotubes give a good performance up to 100 cycles, with capacities of 162, 120 and 105 $mAhg^{-1}$ for current densities of 1, 10 and 40 Ag^{-1} at the 100^{th} discharge, respectively.

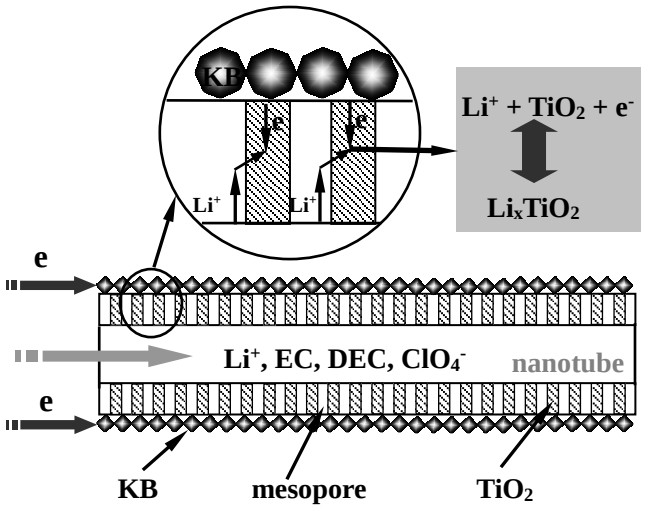

Scheme 1 Transport path of lithium ions and electrons in mesoporous titania nanotube.

The electrode material made of mesoporous titania nanotubes shows a high rate of charge-discharge, which is probably due to the 3 D network structure of mesoporous titania nanotubes. Scheme 1 shows the structure of mesoporous nanotubes and transport path both of lithium ions and electrons. The lithium ions and electrolyte are readily transported in the uniform channels of the mesopores and electrons transport rapidly through the network structure.

In summary, titania nanotubes with mesoporous wall structures, and thus greatly enhanced specific surface areas, have been fabricated within the pores of alumina membranes. The well-defined mesopores in the titania tube walls are packed in a hexagonal manner. This sol-gel templating method is capable of providing precise control of the nanotube dimensions by simply tuning the pore diameter of the alumina membranes and varying the viscosity of the starting sol. After dissolving the alumina membranes, well-ordered uniform nanotubes arrays are obtained via a supercritical drying process. The titania nanotubes with well-ordered mesoporous structures were used as electrode materials in the rechargeable lithium battery which displayed a high rate of

performance. This can be contributed to 3 D network structure of mesoporous titania nanotubes. Such nanostructure provides both electron pathway and lithium ion pathway which are essential for a high rate rechargeable lithium battery. This concept also may also be extended to other positive and negative electrode active materials as an application in energy storage devices.

Experimental

Titania Nanotube Preparation: Titanium tetraisoproxide (TTIP) was used as the titania source and the triblock copolymer, $EO_{20}PO_{70}EO_{20}$ (BASF, Pluronic P123) as the structured directing agent. 0.2 and 0.1 μm anodised aluminium oxide (AAO) membranes were purchased from Whatman (Whatman, Anodisc 13). 50 nm AAO templates were made in our lab using a well known two-step anodization procedure previously reported.[34] A clear sol with a molar composition of 1.0 TTIP: 0.02 P123: 2.4 HCl: 17.5 EtOH was obtained by stirring at room temperature for between 15 min and 3 hrs. Detailed procedure for the preparation of titania sol can be found in our previous work.[35, 36] The sol was further diluted by absolute ethanol (3:1 v/v of ethanol to the initial sol), which decrease the viscosity of the sol from approximate 0.029 to 0.008 cP. AAO membranes were sub-merged into 0.3 ml of the above sol in a small beaker with an inner diameter of about 2.0 cm and aged at room temperature and 60 ºC for one day each. Evaporation-induced self-assembly took place during the ageing process. Most of the volatile species were removed after subsequent annealing at 150 ºC. In order to remove the structural directing agent and crystallize the mesoporous walls, the membranes were subjected to calcination at a temperature of 450 ºC for 3 hrs.

Nanotube Arrays Fabrication in Supercritical Fluids: After the alumina membrane was completely dissolved in 2.0 M NaOH solution, the sample was washed several times with distilled water and ethanol, respectively. The

sample was quickly transferred to a 10 mL high-pressure cell filled with ethanol. The cell was attached via a three-way valve, to a stainless steel reservoir (60 mL). A high-pressure pump (ISCO Instruments, PA) was used to pump CO_2 through the reservoir in to the reaction cell. The cell was pressurized to about 13.8 MPa at room temperature. Ethanol was released from the cell slowly and at last the cell was filled with pressurized CO_2. The cell was heated to about 50 °C and the pressure inside it was maintained at 13.8 MPa for about one hour. Finally, the pressure was decreased to atmosphere pressure very slowly at 50 °C, inducing the transformation of CO_2 from supercritical phase to gas phase.

Titania Nanotubes Characterization: X-ray diffraction (XRD) patterns were recorded in a θ-2θ mode on Philips X'pert PW3710 diffractometer. Nitrogen adsorption-desorption isotherms were collected at 77 K for films scratched from the substrate using Micromeritics Gemini 2375 volumetric analyzer. Barrett, Joyner, and Halenda (BJH) method were used to estimate the pore size and pore-size distribution. Scanning electron microscopy (SEM) was performed on a JEOL JSM-5510 scanning microscope operating at 10 kV. Transmission electron microscopy (TEM) images were collected using JEOL 2000EX microscope operated at 200 kV.

Electrochemical Measurement: For electrochemical measurements, the samples fabricated by using 0.2 μm AAO membranes as hard templates were mixed and ground with 5 wt% Teflon (poly(tetrafluoroethylene)) powder as a binder and 45wt% KB powder as the conductive assistant materials. The mixture was spread and pressed on a 0.25 cm^2 nickel mesh (100 mesh) as the working electrode (WE). The reference (RE) and counter electrode (CE) were prepared by spreading and pressing lithium metals on such a nickel mesh. The electrolyte was 1 M $LiClO_4$ in EC+DMC (EC/DMC=1/1 v/v). Cell assembly was carried out in a glove box under an argon atmosphere.

Galvanostatic discharge-charge was performed in a potential range of 1.0 to 3.0 V (Li^+/Li) under a high rate constant current of 1, 10 and 40 Ag^{-1}. The weight was based on the active materials (TiO_2, excluding KB and Teflon).

Keywords: Titania, mesoporous materials, nanotubes, lithium battery, supercritical fluids

References

[1] M. Adachi, Y. Murata, M. Harada, S. Yoshikawa, *Chemistry Letters* **2000**, 942.
[2] S. Z. Chu, S. Inoue, K. Wada, D. Li, H. Haneda, *J. Mater. Chem* **2003**, *13*, 866.
[3] O. K. Varghese, D. W. Gong, M. Paulose, K. G. Ong, E. C. Dickey, C. A. Grimes, *Adv. Mater.* **2003**, *15*, 624.
[4] M. Adachi, Y. Murata, I. Okada, S. Yoshikawa, *Journal of the Electrochemical Society* **2003**, *150*, G488.
[5] M. D. Wei, Y. Konishi, H. S. Zhou, M. Yanagida, H. Sugihara, H. Arakawa, *J. Mater. Chem.* **2006**, *16*, 1287.
[6] M. D. Wei, Y. Konishi, H. S. Zhou, H. Sugihara, H. Arakawa, *J. Electrochem. Soc.* **2006**, *153*, A1232.
[7] H. S. Zhou, D. L. Li, M. Hibino, I. Honma, *Angew. Chem.-Int. Edit.* **2005**, *44*, 797.
[8] L. Kavan, M. Kalbáč, M. Zukalovä, I. Exnar, V. Lorenzen, R. Nesper, M. Gräetel, *Chem. Mater*., **2004**, *16*, 477.
[9] L. Kavan, J. Rathouský, M. Gräetel, V. Shklover, A. Zukal, *J. Phys. Chem., B* **2000**, *104*, 12012.
[10] L. Kavan, J. Rathouský, M. Gräetel, V. Shklover, A. Zukal, *Micro. Meso. Mater.*, **2001**, *44-45*, 653.
[11] T. Kasuga, M. Hiramatsu, A. Hoson, T. Sekino, K. Niihara, *Advanced Materials* **1999**, *11*, 1307.
[12] Q. Chen, W. Z. Zhou, G. H. Du, L. M. Peng, *Adv. Mater.* **2002**, *14*, 1208.
[13] C. C. Tsai, H. S. Teng, *Chem. Mat.* **2004**, *16*, 4352.
[14] G. K. Mor, O. K. Varghese, M. Paulose, N. Mukherjee, C. A. Grimes, *J. Mater. Res.* **2003**, *18*, 2588.
[15] O. K. Varghese, G. K. Mor, C. A. Grimes, M. Paulose, N. Mukherjee, *J. Nanosci. Nanotechnol.* **2004**, *4*, 733.
[16] S. Z. Chu, K. Wada, S. Inoue, S. Todoroki, *Chem. Mat.* **2002**, *14*, 266.
[17] S. J. Lee, C.; Park, Y., *Chem. Mat.* **2004**, *16*, 4292.
[18] I. J. Park, S.; Hong, J.; Vittal, R.; Kim, K., *Chem. Mat.* **2003**, *15*, 4633.
[19] S. M. Liu, L. M. Gan, L. H. Liu, W. D. Zhang, H. C. Zeng, *Chemistry of Materials* **2002**, *14*, 1391.
[20] Y. C. Zhu, H. L. Li, Y. Koltypin, Y. R. Hacohen, A. Gedanken, *Chemical Communications* **2001**, 2616.
[21] M. Adachi, I. Okada, S. Ngamsinlapasathian, Y. Murata, S. Yoshikawa, *Electrochemistry* **2002**, *70*, 449.
[22] T. Y. Peng, A. Hasegawa, J. R. Qiu, K. Hirao, *Chem. Mat.* **2003**, *15*, 2011.
[23] B. Yao, D. Fleming, M. A. Morris, S. E. Lawrence, *Chem. Mat.* **2004**, *16*, 4851.
[24] W. S. Chae, S. W. Lee, Y. R. Kim, *Chem. Mat.* **2005**, *17*, 3072.
[25] A. Yamaguchi, F. Uejo, T. Yoda, T. Uchida, Y. Tanamura, T. Yamashita, N. Teramae, *Nature Materials* **2004**, *3*, 337.
[26] L. F. Liang, H. F. Xu, Q. Su, H. Konishi, Y. B. Jiang, M. M. Wu, Y. F. Wang, D. Y. Xia, *Inorganic Chemistry* **2004**, *43*, 1594.
[27] Z. Yang, Z. Niu, X. Cao, Z. Yang, Y. Lu, C. C. Han, *Angew. Chem.-Int. Edit.* **2003**, *42*, 4201.
[28] D. H. Wang, R. Kou, Z. L. Yang, J. B. He, Z. Z. Yang, Y. F. Lu, *Chem. Commun.* **2005**, 166.
[29] D. Grosso, G. Illia, E. L. Crepaldi, B. Charleux, C. Sanchez, *Adv. Funct. Mater.* **2003**, *13*, 37.
[30] J. R. Matos, M. Kruk, L. P. Mercuri, M. Jaroniec, L. Zhao, T. Kamiyama, O. Terasaki, T. J. Pinnavaia, Y. Liu, *J.*

Am. Chem. Soc. **2003**, *125*, 821.
[31] H. Y. Wang, T. Abe, S. Maruyama, Y. Iriyama, Z. Ogumi, K. Yoshikawa, *Adv. Mater.* **2005**, *17*, 2857.
[32] M. Wagemaker, A. P. M. Kentgens, F. M. Mulder, *Nature* **2002**, *418*, 397.
[33] L. Kavan, M. Gratzel, J. Rathousky, A. Zukal, *J. Electrochem. Soc.* **1996**, *143*, 394.
[34] D. Erts, B. Polyakov, B. Dalyt, M. A. Morris, S. Ellingboe, J. Boland, J. D. Holmes, *J. Phys. Chem. B* **2006**, *110*, 820.
[35] K. Wang, M. A. Morris, J. D. Holmes, *Chem. Mat.* **2005**, *17*, 1269.
[36] K. Wang, B. Yao, M. A. Morris, J. D. Holmes, *Chem. Mater.* **2005**, *17*, 4825.

Supplementary information

SI figure 1 The sol viscosity gives an important influence on the final nanostructure within AAO as shown in the following SEM image of titania nanorods within AAO. These nanorods were prepared from sols with viscosity of approximately 0.025 cP.

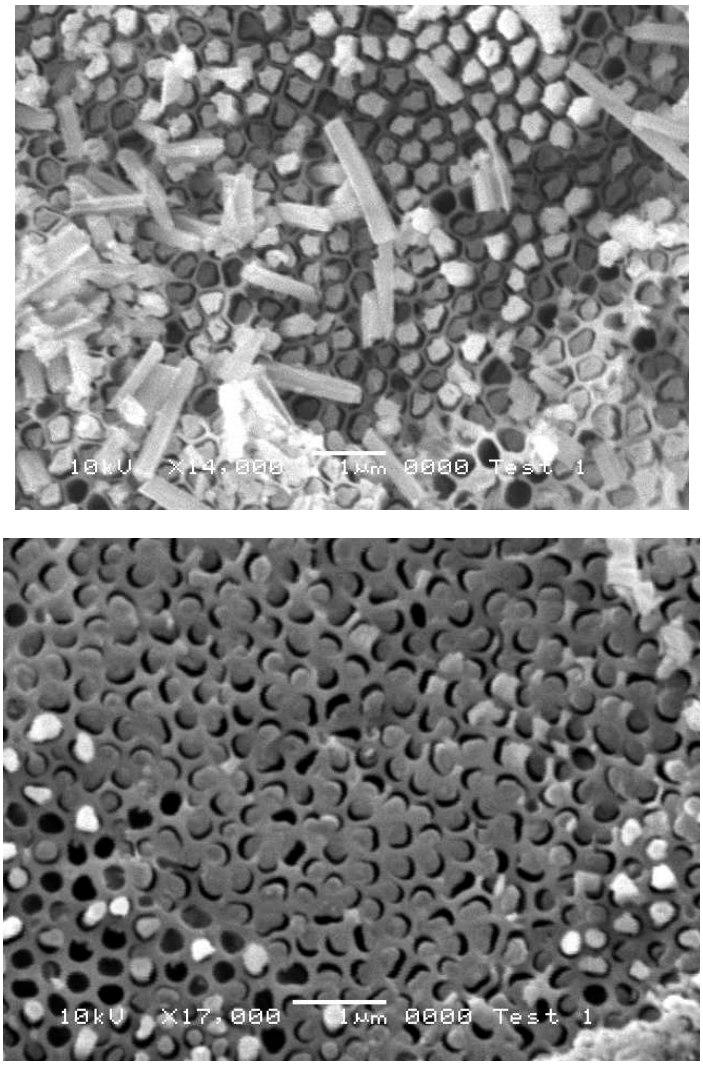

SI Figure 2 Scanning electron microscopy images of titania nanotubes dried up in air after the dissolving of the alumina membranes. Without supercritical CO_2 treatment, all of the nanotubes are entangled together to form nanotubes bundles due to the surface tension force subjected to the tubes during the drying up process.

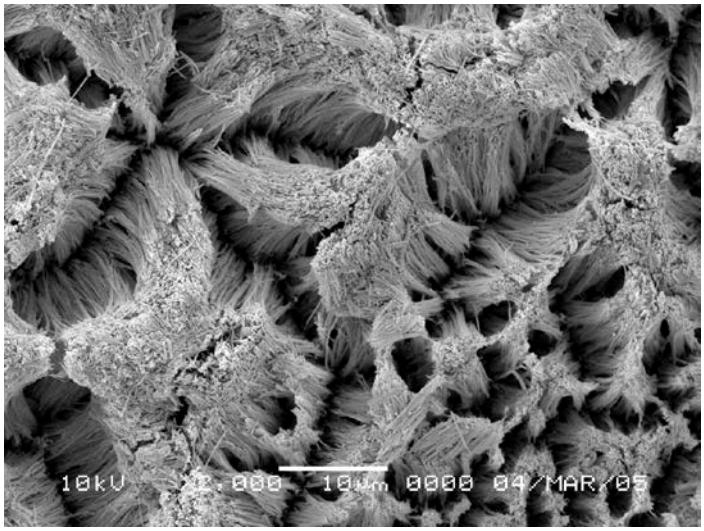

(a)

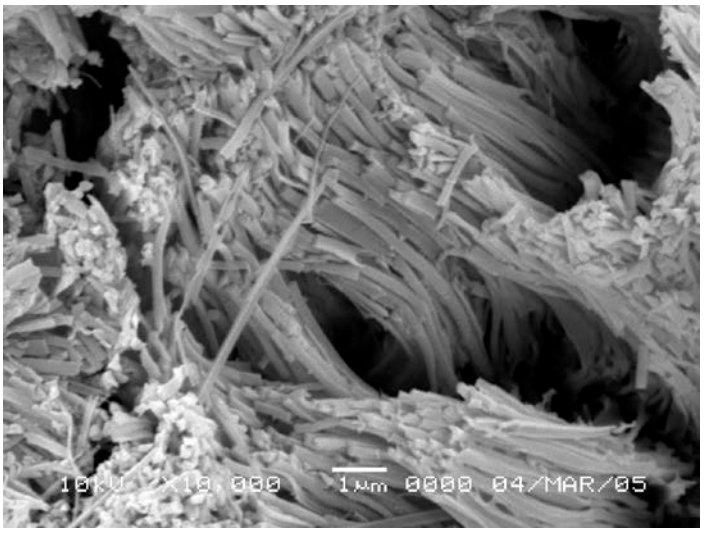

(b)

SI Figure 3 High-angle PXRD pattern of TiO_2 nanotubes calcined at 450 ºC showing the diffraction of nanosized anatase.

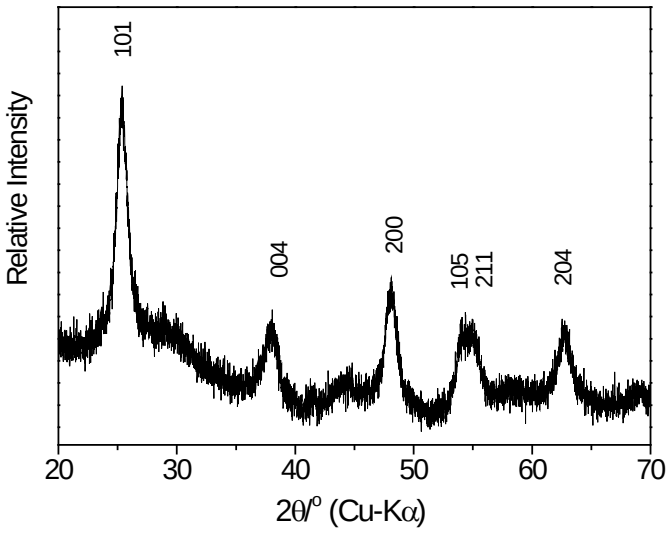

SI figure 4 The first cycle charge-discharge profiles of KB in the potential range from 1.2 to 3 V (versus Li+/Li) with the current density of 1 and 10 A g-1 based on active KB.